SUPPRESSION OF THE 1MHZ BEAM CURRENT MODULATION IN THE LEDA PROTON SOURCE

Pascal Balleyguier, CEA, Bruyeres-le-Chatel, France
Joseph Sherman, Thomas Zaugg, LANL, Los Alamos, USA

Abstract

Earlier operation of a microwave proton source exhibited an approximate 1-MHz modulation in the beam current. This oscillation could cause instabilities at higher energy in the linac, as the low-level RF control for linac operation rolls off at 200 kHz. Tests on a dummy load showed the modulation was created by the magnetron itself. Since the magnetron exhibits better behavior at higher levels, an RF power attenuator was inserted to force the magnetron to run at a higher power. This attenuator is made of two antennas plunged a quarter of guided wavelength apart in the waveguide and connected to dummy loads by a coaxial line. Magnetron operation at the higher power level gives a beam current spectrum free of the 1-MHz modulation, showing the coherent beam noise is not generated by plasma chamber phenomena.

1 MAGNETRON CHARACTERIZATION

Recent operations of the LEDA proton source [1-2] showed that the beam current was modulated in amplitude at a frequency of approximately 1 MHz. Earlier works already mention this kind of problem [3]. In the future downstream accelerator, any beam current variation would result in a varying beam-loading and could cause serious RF field instabilities. A challenge was to find out how to get rid of this modulation.

Previous measurements showed that the modulation was present in the 2.45 GHz RF power injected in the source plasma. In order to tell if the beam modulation was caused by a plasma resonance or by the RF generator itself, we connected the magnetron to a dummy load and measured the RF spectrum via a directional coupler (fig. 1). At 680 W (typical RF level for this application), its output still exhibited a strong 1 MHz modulation. Varying the RF power resulted in different spectra, and we established that the spectrum was completely free of modulation at higher powers, (see for example, the spectrum for 975 W in figure 2). The plot on figure 3 shows that the modulation strongly depends on the magnetron output power. The sideband effect is probably caused by a resonance in the tube.

Unfortunately, the useful power range for our ion source operation (500 to 800 W) is in the middle of this resonance. The good behavior of the magnetron above 800 W suggests to run it at a higher power range in order to get rid of the modulation. The magnetron can provide 750 to 1200 W of power and one third of this power can be dissipated in a power coupler.

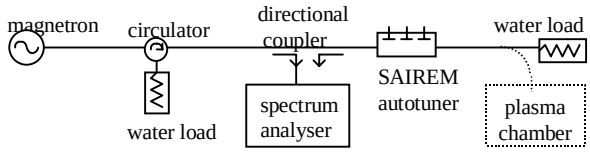

Figure 1: Measurement of the magnetron RF spectrum.

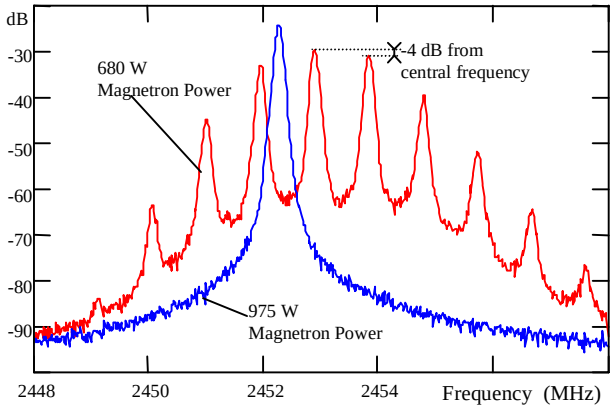

Figure 2: Magnetron power spectra at 680 and 975 W

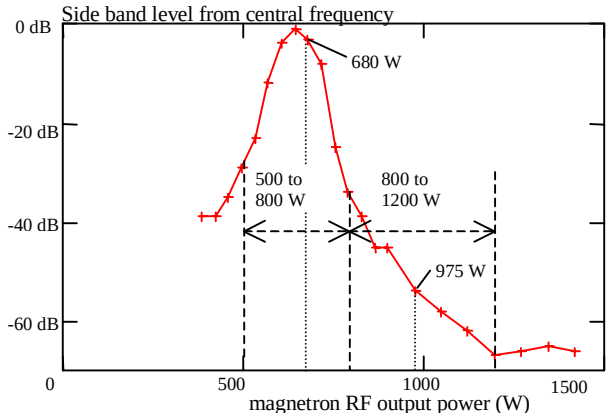

Figure 3: Sideband level vs. RF power

2 POWER EXTRACTOR

The device we need is an RF attenuator that transmits 66.7% of the input power. Such an attenuator (-1.78 dB, dissipating up to 400 W on a WR284 waveguide at 2.45 GHz), is not a standard product and would have a high price and a long delay if ordered from a manufacturer. Therefore, we decided to build it within the laboratory. It is easy to extract some RF power from a waveguide by inserting an electric antenna in the high electric field region and connecting the antenna to a coaxial load. The antenna length can be adjusted to attain a given coupling value, but this generates a local mismatch and results in

a reflected wave in the guide. If the power extractor consists of two identical antennas a quarter of guided wavelength apart, the two reflected waves are out of phase and approximately cancel each other. Moreover, as each of the antennas has to extract only 1/6 of the input RF power, they can be smaller in size, and this also reduces the mismatch effects of the device.

2.1 Single antenna pick-up theory

Consider a $\lambda_g/4$ long piece of lossless waveguide. The transfer coefficient between the input and output planes is the complex number *i*. Introducing an antenna in the middle of this device can lower the transfer coefficient modulus, and also alter the phase by $\Delta\varphi$. The original $\pi/2$ phase can be restored (fig. 4) by shifting the reference planes by :

$$\Delta l = -\frac{\Delta\varphi}{2\pi}\lambda_g . \quad (1)$$

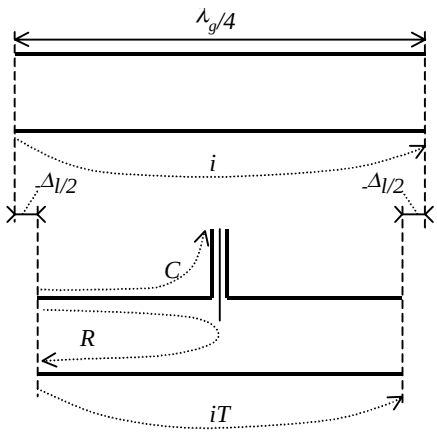

Figure 4: Single antenna pick-up. The reference planes have been displaced in order to keep the forward transfer coefficient a purely imaginary number.

The transfer coefficient of this "single antenna pick-up" is *iT, T* being a positive real number. In the coaxial line, the reference plane is chosen so the coupling coefficient *C* is also a positive real number. The antenna causes a reflected wave in the waveguide with an a priori arbitrary phase. Let *R* be the complex reflection coefficient seen from the input reference plane. Energy conservation implies:

$$|R|^2 + C^2 + T^2 = 1 . \quad (2)$$

As seen in the following section, *R* must also be a real number. That physically means that the reflection coefficient phase on the antenna is null if seen from a reference plane $\lambda_g/8$ upstream from the antenna (Δl is neglected here). In other words, the reflection phase is $\pm\pi/2$ if the reference plane is on the antenna itself.

2.2 Dual antenna pick-up theory

The dual antenna pick-up is obtained by cascading two devices identical to the single antenna pick-up described above (fig.5). We will assume that the inter antenna distance ($\lambda_g/4+\Delta l$) is large enough that the field patterns perturbation caused by one antenna is not seen by the other one. If the perturbation was non-negligible, the antennas could be separated by an additional integer number of $\lambda_g/2$.

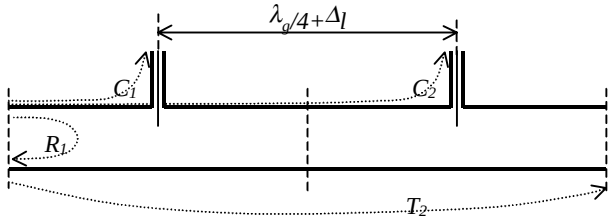

Figure 5: Dual antenna pick-up

Let T_2 be the global transfer coefficient. The incoming wave is multiplied by *iT* by the first antenna and *iT* again by the second antenna, giving $-T^2$ as the first term in T_2. The reflection on the second antenna creates a wave that is partially reflected again by the first antenna. At this point (medium reference plane), the transfer coefficient is $iT.R^2$. Going through the second antenna, this secondary waves reaches the output plane with a transfer coefficient multiplied again by *iT*, resulting in $iT.R^2.iT=-T^2R^2$. Considering now the wave doing one more round trip between the two antennas results in $iT.R^4.iT=-T^2R^4$. And so on... The summation of all these waves gives the actual transmitted wave:

$$T_2 = -T^2 + \sum_{k=1}^{\infty} -T^2R^{2k} = -\frac{T^2}{1-R^2} . \quad (3)$$

The same kind of argument gives the global reflection coefficient R_1, and the two coupling factors C_1 and C_2:

$$R_1 = R + \sum_{k=1}^{\infty} -T^2R^{2k-1} = R\left(1-\frac{T^2}{1-R^2}\right), \quad (4)$$

$$C_1 = C + \sum_{k=1}^{\infty} -iTCR^{2k-1} = C\left(1+i\frac{RT}{1-R^2}\right), \quad (5)$$

$$C_2 = iTC\sum_{k=1}^{\infty} -iTCR^{2k} = i\frac{TC}{1-R^2} . \quad (6)$$

Conservation of energy implies:

$$|R_1^2| + |C_1^2| + |C_2^2| + |T_2^2| = 1 \quad (7)$$

With equations (2) to (6), (7) can easily be proven if *R* is a pure real number. It is more difficult to prove the reciprocal proposition, but one can easily be convinced (by some numerical tests) that equation (7) can only be true if *R* is real, as mentioned in previous section.

Equation (4) shows that, as expected, the global reflection coefficient has been reduced by the second antenna, though it has not been completely cancelled because the second antenna receives a signal that has been already attenuated by the first one. For the same

reason, the two coupled output coefficients $|C_1|$ and $|C_2|$ are roughly equal to *C*.

The goal is to reach a specific transfer value $|T_2|$. From equation (3), one can see that T^2 must be chosen slightly greater than $|T_2|$, as R^2 is expected to be much smaller than unity. To be more precise, the link between *R* and *T* is needed, or equivalently because of equation (1), the link between *R* and *C*. While this link cannot easily be predicted, it can be measured experimentally.

2.3 Realization

A single antenna has been installed in the waveguide. A 9 mm hole has been drilled in the upper wall guide, and a connector socket (N type) fixed on the external side in a way that the socket pin would make an electrical antenna within the guide. As this antenna proved to be too short, a screw was placed in the socket pin (fig. 6) to increase the coupling coefficient *C*.

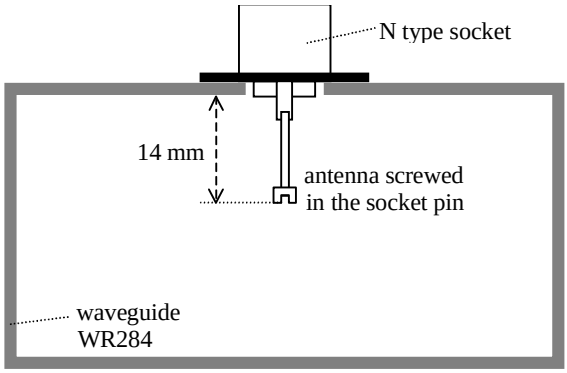

Figure 6: Mechanical design of the pick-up antenna. The two antennas are 51 mm apart.

After testing different antenna lengths, we established that the link between R and C was approximately:

$$C = 0.85 \cdot R + 0.18 . \qquad (8)$$

The goal value for C was computed numerically from equations (2)(3)(8) and from T_2^2=0.667: C=0.414. With a 14 mm antenna, we measured C≈0.399, and considered it was close enough to the goal. The phase shift introduced by a single antenna on the transmission coefficient was measured by comparing the waveguide phase transmission successively with and without the antenna: Δφ=11°. From eq.(1), the waveguide width and the operating frequency (a=72 mm, f=2.45 GHz), we computed the correct distance between the antennas:

$$\lambda_g/4+\Delta l=233/4-7\approx 51 \text{ mm}.$$

After installing the second antenna at this distance, we measured the dual antenna device characteristics:

$|R_1|$=0.028 (-30.8 dB), $|C_1|$=0.435 (-7.22 dB),
$|C_2|$=0.350 (-9.11 dB), $|T_2|$=0.822 (-1.70 dB).

The power transmission coefficient ($|T_2^2|$=0.675) is close to the design value (0.667), and the reflection coefficient is even better than predicted (SWR =1.06): the objective of power extraction without important mismatching has been reached. When operating the magnetron up to 1200 W, the loads have to dissipate up to 227 and 147 W, respectively. The loads installed can hold up to 250 W RF power, and a fan has been installed to cool them.

3 CONCLUSION

We tested the source performance with the same RF power delivered to the plasma chamber with and without the power extractor installed. With power extractor, the magnetron delivers 1010 W and the plasma chamber sees 682 W. The current source spectrum is now free of any 1 MHz modulation and cannot be distinguished from the background noise (fig. 7).

We proved that the 1 MHz modulation on the source current was entirely due to the magnetron, and was not generated by any phenomenon in the plasma chamber, and we found a simple and efficient way to get rid of this modulation.

The source current noise spectrum is now low enough to accurately identify the influence of various ion source parameters on the current spectrum.

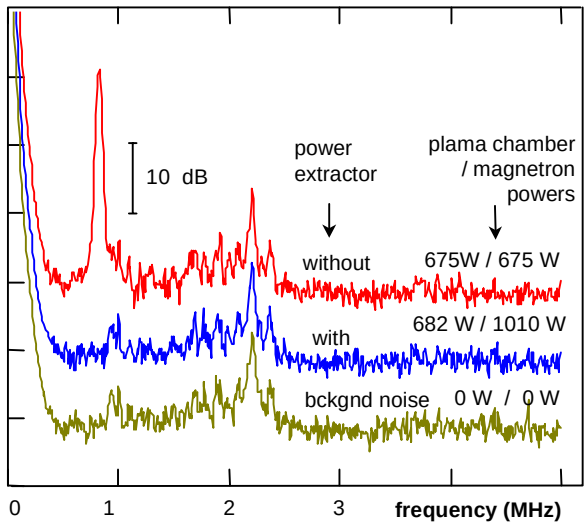

Figure 7: Current spectra comparison at constant RF power in the plasma chamber.
(For clarity, the "without" and "with" curves have been shifted up by 20 and 10 dB respectively).

REFERENCES

[1] J.Sherman et al., "Status report on a DC 130 mA 75 keV proton injector", Rev. of Sci. Instr., Vol 69, p 1003, (1998).

[2] J. Sherman et al., "A DC Proton Injector for Use in High-Current CW Linacs", submitted to European Particle Accelerator Conference, Stockholm, 22-26 June 1998.

[3] I. Soloshenko, "Physics of Ion Beam Plasma and Problems of Intensive Ion Beam Transportation", Rev. Sci. Instrum., Vol 67-4, p. 1646(1996).